Supplemental Material

Assay Conditions Influence Affinities of Rat Organic Cation Transporter 1: Analysis of Mutagenesis in the Modeled Outward-facing Cleft by Measuring Effects of Substrates and Inhibitors on Initial Uptake.

Valentin Gorboulev, Saba Rehman, Christoph M. Albert, Ursula Roth, Marleen J. Meyer, Mladen V. Tzvetkov, Thomas D. Mueller, and Hermann Koepsell

Molecular Pharmacology

Supplemental Table 1

Comparison of effects of mutations in rOCT1 on IC_{50} values determined for inhibition of MPP^+ uptake by TEA^+ with apparent K_m values of TEA^+ uptake. Initial uptake measurements of 0.1 µM MPP^+ in the presence of varying concentrations of TEA^+ were performed at 37°C in stably-transfected HEK293 cells and the IC_{50} values for inhibition by TEA^+ by fitting the Hill equation to the data. Mean values ± S.D. of 3-5 separate experiments are shown. The compiled data including the determined Hill coefficients are shown in Supplementary Fig. 4. The apparent K_m values for TEA^+ uptake (mean values ± SD) presented in Table 3 of the manuscript are shown for comparison.

rOCT1	TEA^+ IC_{50} [µM]	Transport of TEA^+ app.K_m *[µM]*
Wildtype	42±7.1$^{\Delta}$	67±9.9
F160A	53±3.0	57±8.3
F160Y	280±35***, $^{\Delta\Delta\Delta}$	84±22
W218F	239±50 ***	230±28 ***
W218Y	84±16 $^{\#\#}$	61±7.2
W218L	129±23 ***	no uptake
Y222F	20±1.5 $^{\#\#, \Delta\Delta\Delta}$	55±11
T226A	22±3.5 $^{\#\#, \Delta\Delta\Delta}$	60 ±7.7
R440K	32±6.2	32±6.0 $^{\#\#}$
L447F	44±8.8 $^{\Delta\Delta\Delta}$	167±23***
L447Y	96±16 *	80±6.1
D475E	53±8.1 $^{\Delta\Delta\Delta}$	19±2.9***

*P<0.05, ***P<0.001 difference to wildtype, ANOVA and Tukey test; $^{\#\#}$P<0.01 difference to wildtype, Student´s t-tests; $^{\Delta}$P<0.05, $^{\Delta\Delta\Delta}$P<0.001 difference to apparent K_m for TEA uptake, Student´s t-test.

Michaelis-Menten equation

$$Y = Bottom + (Top - Bottom) - \left(\frac{(Top - Bottom) \times 10^{X}}{Km + 10^{X}}\right)$$

Hill equation

$$Y = Bottom + (Top - Bottom) - \left(\frac{(Top - Bottom) \times (10^{X})^{N}}{Km^{N} + (10^{X})^{N}}\right)$$

Two-site-competition

$$Y = Bottom + (Top - Bottom)\left[\frac{Fraction\ 1}{1 + 10^{X - Log\ IC50\_1}} + \frac{1 - Fraction\ 1}{1 + 10^{X - Log\ IC50\_2}}\right]$$

Supplemental Fig. 1. Equations which were applied for calculation of apparent *K*m values from substrate replacement curves (Figs. 3, 4, Supplemental Fig. 2) and of IC_{50} values from inhibition curves (Figs. 2, 5, 6, 7, Supplemental Figs. 3, 4). Y represents uptake of [^{3}H]MPP^{+} or [^{14}C]TEA^{+}, X represents the logarithmus of unlabeled substrate (MPP^{+} or TEA^{+}) or of inhibitor (TBuA^{+}, TPeA^{+} or corticosterone). Top indicates the uptake of [^{3}H]MPP^{+} or [^{14}C]TEA^{+} without addition of unlabeled substrate or without addition of inhibitor. In the presented experiments this value has been normalized to 1. Bottom indicates uptake of [^{3}H]MPP^{+} or [^{14}C]TEA^{+} in the presence of the highest concentration of substrate or inhibitor, N represents the Hill coefficient. In the two-site-competition model it is assumed that unlabeled MPP^{+}, TEA^{+}, TBuA^{+}, TPeA^{+} or corticosterone inhibit transport of radioactively labeled [^{3}H]MPP^{+} by interacting with two inhibitory sites. Fraction 1 indicates the fraction of [^{3}H]MPP^{+} uptake which is inhibited with the half maximal concentration *IC*50_1 whereas the remaining fraction of [^{3}H]MPP^{+} uptake is inhibited with *IC*50_2.

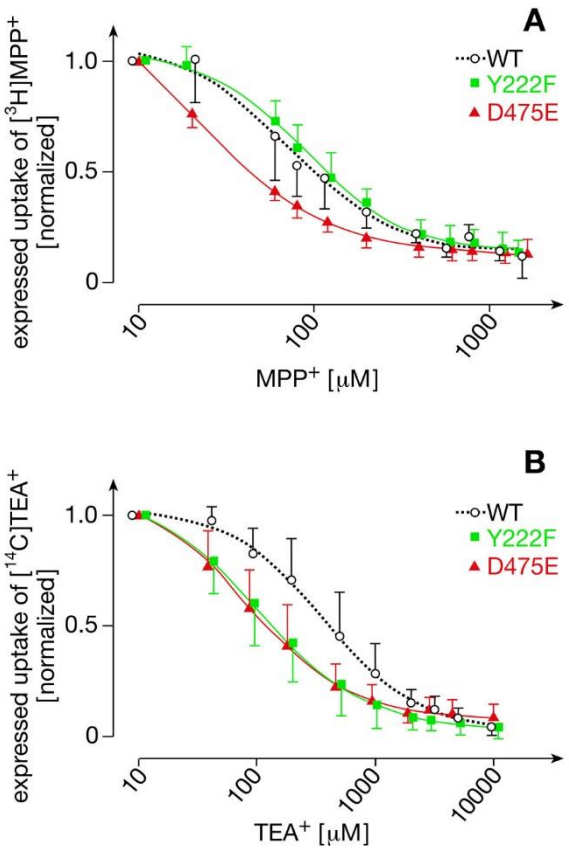

Supplemental Fig. 2. Determination of apparent K_m values for uptake of MPP^+ and TEA^+ in confluent HEK293, which were stably transfected with wildtype rOCT1 or rOCT1 mutants. Uptake of radioactively labeled MPP^+ (A) or TEA^+ (B) was measured after 2 min-incubation at 37°C. The data were normalized to uptake of 10 µM MPP^+ or 10 µM TEA^+. Mean values ± S.D of 3 independent experiments are shown. Curves were obtained by fitting the Michaelis-Menten equation to the data.

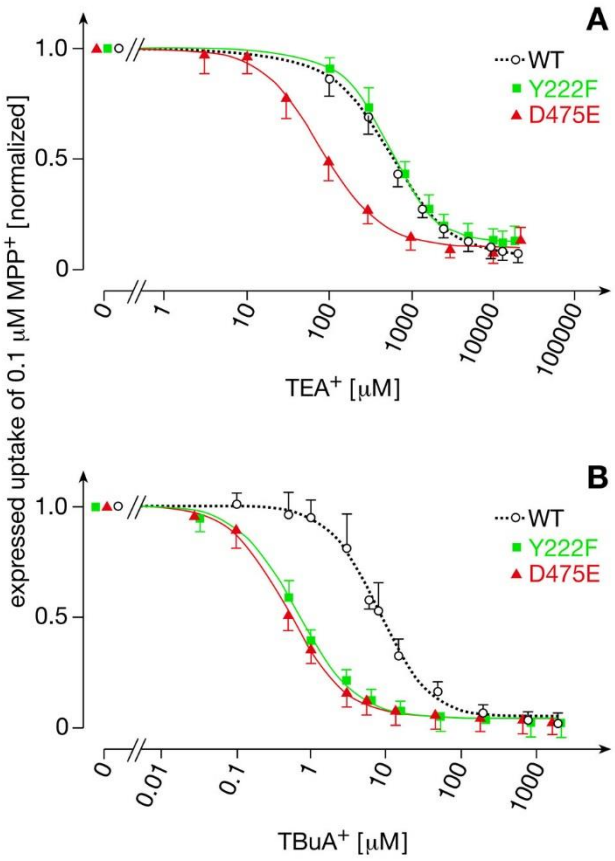

Supplemental Fig. 3. Determination of IC_{50} values for inhibition of uptake of 0.1 µ*M* MPP^+ by TEA^+ or $TBuA^+$ in confluent HEK293, which stably expressed wildtype rOCT1 or mutants thereof. Uptake of radioactive MPP^+ in the presence of different concentrations of TEA^+ (A) or $TBuA^+$ (B) was measured after 2 min-incubation at 37°C. Data were normalized to uptake of 0.1 µ*M* MPP^+ in the absence of TEA^+ and $TBuA^+$. Mean values ± S.D of 3 independent experiments are shown. The curves were obtained by fitting the Hill-Equation to the data.

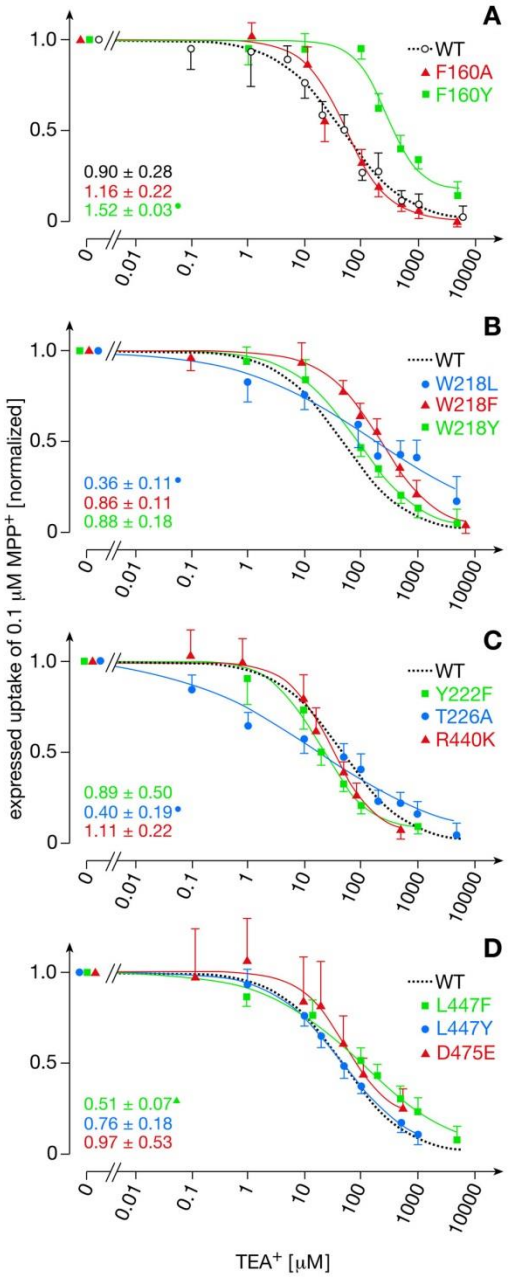

Supplemental Fig. 4. Impact of mutations in rOCT1 on inhibition of initial uptake of 0.1 µM MPP^+ by TEA^+ measured in dissociated HEK293 cells. 1 s- or 5 s-uptake measurements (5 s in case of mutant D475E) of 0.1 µM MPP^+ into HEK293 cells stably transfected with wildtype rOCT1 or rOCT1 mutants were perfomed at 37°C in the absence of TEA^+ and in the presence of various TEA^+ concentrations. The data were normalized to MPP^+ uptake in the absence of TEA^+. Mean values ± S.D. of 3 experiments are indicated. The curves were obtained by fitting the Hill equation to the compiled data. Mean values ± S.D. of Hill coefficients are indicated which were determined by fitting the Hill equation to individual experiments. •$P<0.05$ for difference to the Hill coefficient of wildtype rOCT1 determined by Student´s t-test. ▲Mean value of Hill coefficient is more than 2×S.D. below one.

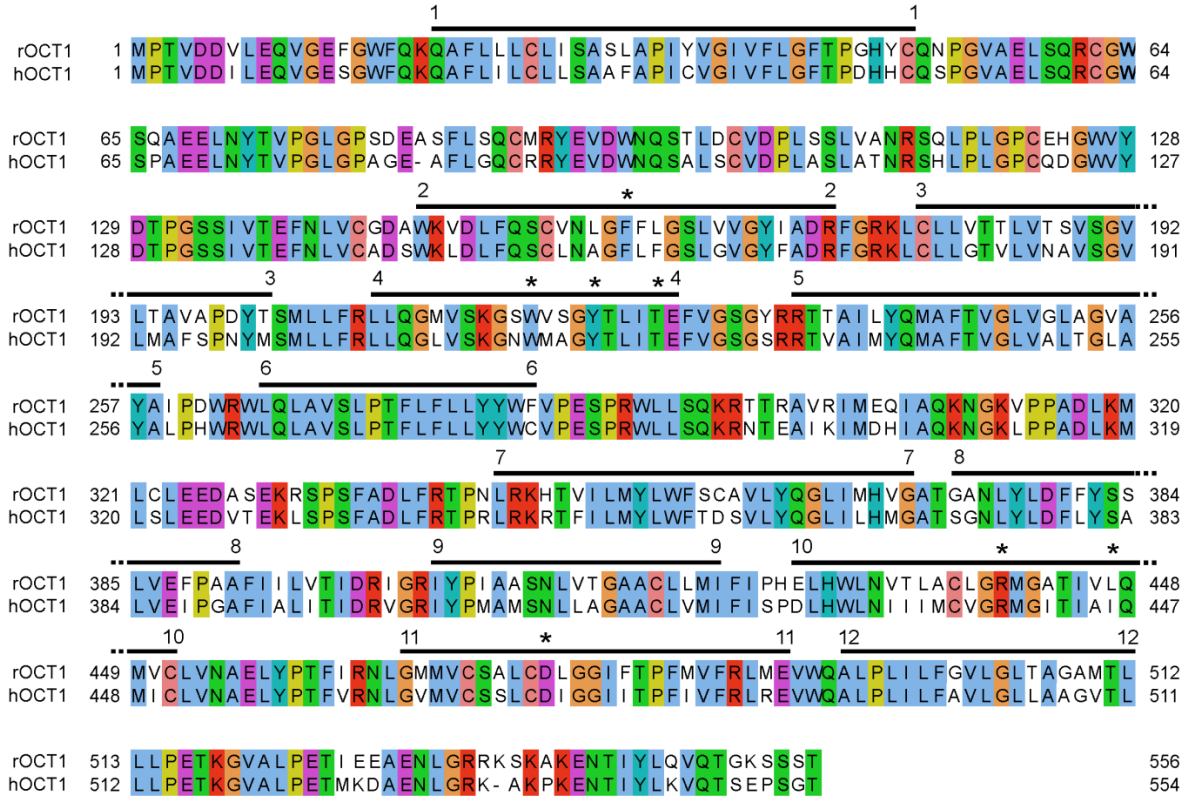

Supplemental Fig. 5. Amino acid sequence alignment of rOCT1 (uniprot code Q63089) and hOCT1 (uniprot code O15245). The alignment was performed using ClustalOmega and visualized using JalView version 2.10.1. Amino acids were color-coded using the Clustalx coloring scheme and modulating the color intensity by the degree of conservation. Twelve predicted transmembrane helices are indicated by black lines and numbered accordingly. The residues mutated in this study are marked by asterisks.

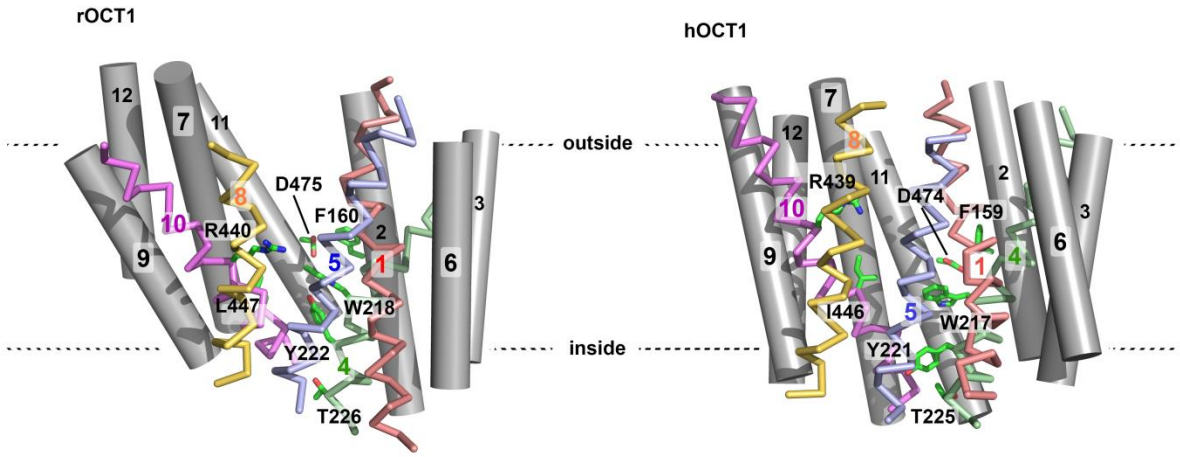

Supplementary Fig. 6. Cartoon representation of 3D homology models of rOCT1 and hOCT1 in the presumed outward-open conformations modeled by different approaches as described earlier (Gorbunov et al., 2008; Dakal et al., 2017). Both models were structurally superimposed and are shown in the identical orientation to allow for comparison. The side chains of residues Phe160, Trp218, Tyr222, Thr226, Arg440, Leu447 and Asp475 of rOCT1 as well as the equivalent residues in hOCT1 (one letter code is used in the figure for better visability, please note, that numbering is off by 1 due to a one-amino acid insertion in hOCT1) are shown in stick representation indicating that all residues superimpose quite well within the accuracy limits of the 3D homology models. As both models were derived using different structure template sets employing rather different modeling approaches, the high similarity strongly indicates that both models can be used equivalently for analysis and interpretation of functional data.

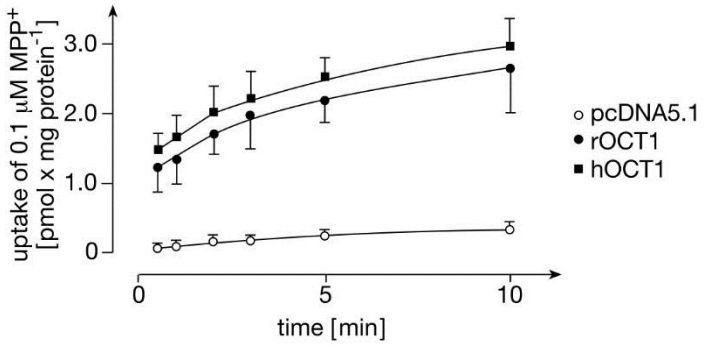

Supplementary Fig. 7. Time courses of MPP^+ uptake into confluent monolayers of HEK293 cells stably transfected with rOCT1, hOCT1 or control plasmid pcDNA5.1 that were grown on plastic dishes. Cloning of hOCT1 in vector pcDNA5.1 and generation of HEK293 cells have been described earlier (Tzvetkov et al., 2012). Confluent monolayers were incubated for different time periods at 37°C in Mg-Ca-PBS containing 0.1 µM MPP^+ traced with [^{3}H]MPP^+. Uptake was stopped by washing the monolayers with ice-cold PBS. The cells were solubilized with 4 M guanidine thiocyanate and analysed for radioactivity. Mean values ± S.D. of four independent experiments are shown.